NASA Contractor Report 194468

Equations for Estimating the Strength of TV Signals Scattered by Wind Turbines

David A. Spera
Sverdrup Technology, Inc.
2001 Aerospace Parkway
Brook Park, Ohio

and

Dipak L. Sengupta
University of Detroit Mercy
Detroit, Michigan

May 1994

Prepared for
Lewis Research Center
Under Contract NAS3–25266

National Aeronautics and
Space Administration

EQUATIONS FOR ESTIMATING THE STRENGTH OF TV SIGNALS SCATTERED BY WIND TURBINES

David A. Spera
Sverdrup Technology, Inc.
Lewis Research Center Group
2001 Aerospace Parkway
Brook Park, Ohio 44142

and

Dipak L. Sengupta
University of Detroit Mercy
Detroit, Michigan 48221

Introduction

During the late 1970's and early 1980's, concerns about the potential interference of wind turbine generators with electromagnetic communication signals led to a series of research studies, both in the laboratory and in the field, conducted by the staff of the University of Michigan Radiation Laboratory. These studies were sponsored by organizations such as the U.S. Department of Energy (Refs. 1 - 7), the Solar Energy Research Institute (Refs. 5 - 8), and private developers of wind power stations (Refs. 9 and 10). Research objectives were to *identify the mechanisms* by which wind turbines might adversely affect communication signals, *estimate the severity* of these effects for different types of signals (e.g. television, radio, microwave, and navigation), and *formulate mathematical models* with which to predict the sizes of potential interference zones around wind turbines and wind power plants. This work formed the basis for preliminary standards on assessing electromagnetic interference (EMI) by wind turbines (Ref. 11).

With the current renewal of interest in wind energy projects, it is appropriate that the many experimental and analytical aspects of this pioneering work be reviewed and correlated. The purpose of this study is to combine test data and theory from previously published and unpublished research reports into a unified and consistent set of equations which are useful for estimating potential levels of television interference from wind turbines. To be comprehensive, these equations will include both horizontal-axis and vertical-axis wind turbines (HAWTs and VAWTs), blade configuration parameters (e.g. number, size, material, twist, and coning), signal frequency and power, and directional characteristics of the receiving antenna.

The approach that is followed in this report is as follows: First, some basic equations that describe electromagnetic signals with interference are presented without detailed derivations, since the latter are available in the references. Minor changes in terminology are made for purposes of consistency. Next, the concept of a *signal scatter ratio* is introduced, which defines the fraction of the signal impinging on a wind turbine that is scattered by its blades onto a nearby receiver. Equations from references are modified for the calculation of experimental scatter ratios (from measured signals containing interference) and idealized scatter ratios (from rotor characteristics and relative locations of the transmitter, the turbine, and the receiver). Experimental and idealized scatter ratios are then calculated and compared for 75 cases from the literature, in which TVI measurements were made around a variety of wind turbines (Fig. 1). An empirical equation is then defined for estimating the probability that an actual scatter ratio will differ from an idealized ratio by a given amount. Finally, a sample calculation of the size of a potential TV interference zone around a hypothetical wind power station is presented.

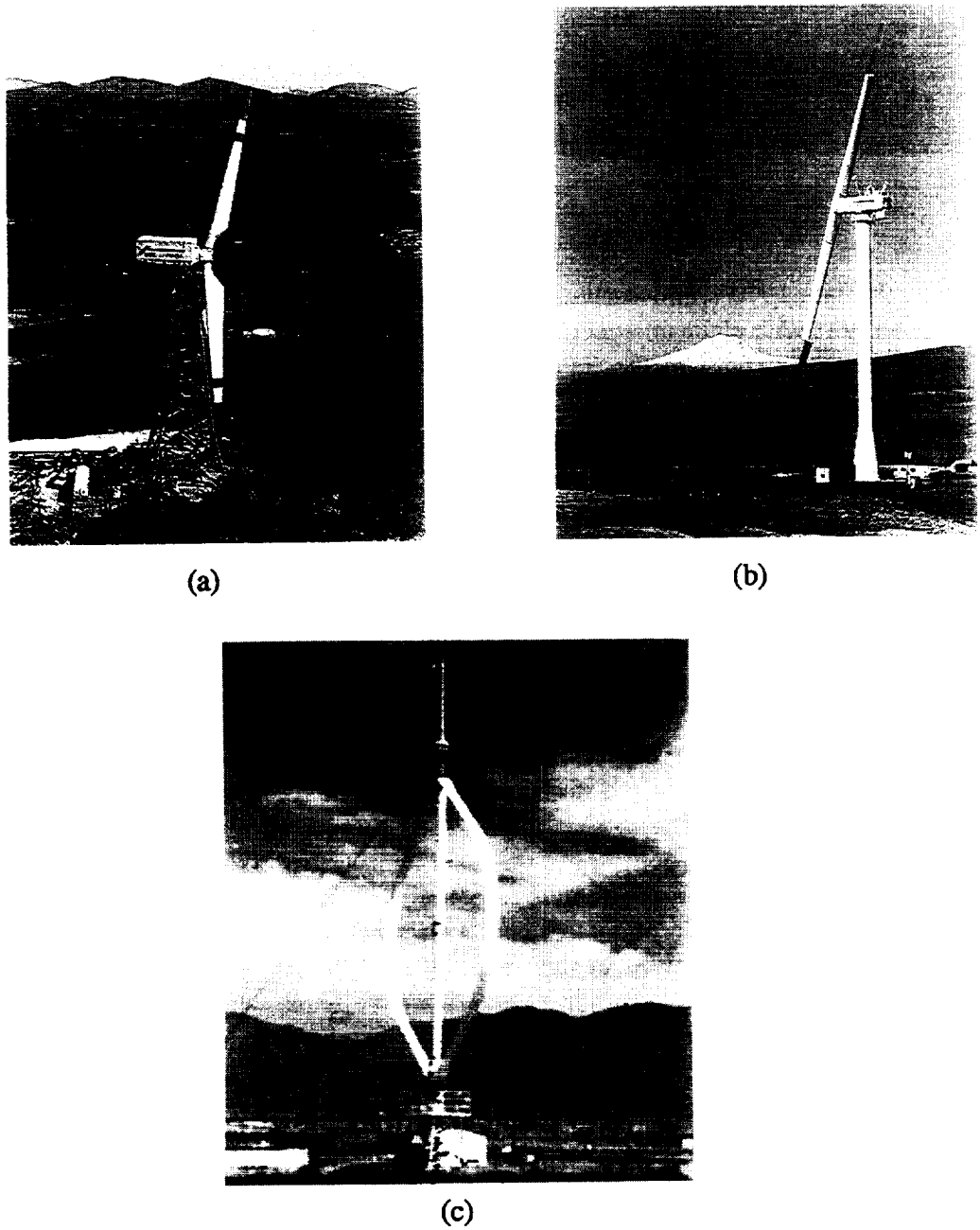

Figure 1. Experimental wind turbines around which some of the first research on the scattering of electromagnetic signals by wind turbine blades was conducted in the late 1970's and early 1980's. (a) The DOE/NASA 2.0-MW Mod-1 HAWT near Boone, NC. (b) The DOE/NASA 2.5-MW Mod-2 HAWT near Goldendale, WA. (c) The DOE/Sandia 500-kW 17-m Darrieus VAWT near Albuquerque, NM.

Basic Equations

A general model is developed and presented in References 1 and 5 of the essential mechanism by which a wind turbine can produce electromagnetic interference, and the following discussion originates in these references. Figure 2 illustrates the field conditions under which a wind turbine may cause EMI. A transmitter (*T*) sends a *direct signal* to receivers (*R*) and to a wind turbine *(WT)* that may be of either the horizontal- or vertical-axis configuration (HAWT or VAWT). The rotating blades of the turbine produce and transmit a *scattered signal.* Thus, the receivers may acquire two signals simultaneously, with the scattered signal causing EMI because it is delayed and/or distorted. Signals reflected in a manner analogous to mirror reflection are termed *back-scattered.* As shown in the figure, about 80 percent of the region around the turbine is the *backward-scatter zone.* On the other hand, signal scattering that is analogous to shadowing is termed *forward scattering*, and about 20 percent of the region around a turbine is the *forward-scatter zone.*

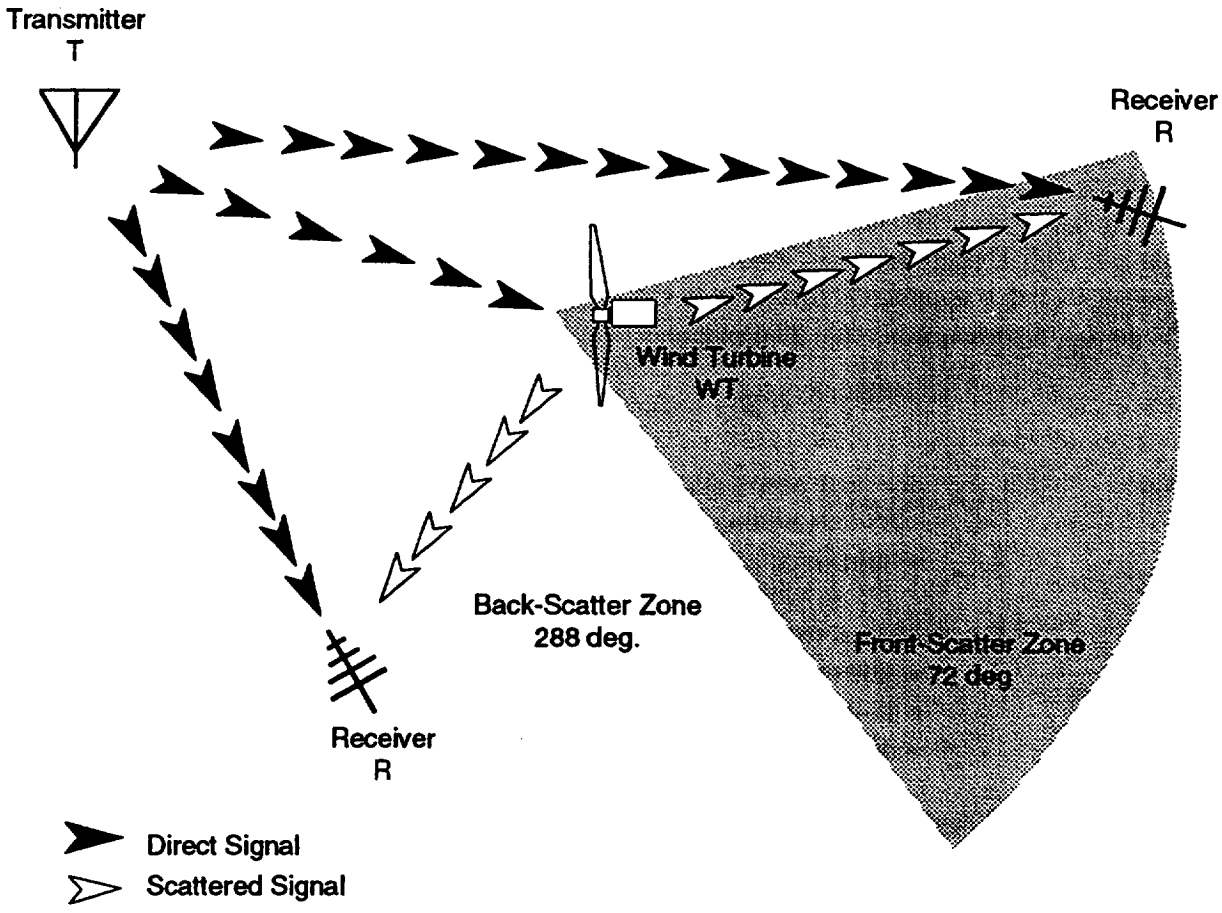

Figure 2. Schematic plan view of the relative positions of a transmitter, receivers, and a wind turbine that may produce EMI. Interference is caused by the simultaneous reception of both the direct and the scattered signals, the latter being delayed and/or distorted.

The envelope of the total *electric field strength* of the ambient signal, E, surrounding a receiving point, R, can be written as

$$|E_R|_{envelope} = |E_{R,D}|\,[1 + m_E f_m(t)] \tag{1a}$$

$$m_E = \frac{|E_{R,S}|}{|E_{R,D}|} \tag{1b}$$

where
E_R = field strength at the receiver of the total signal (mV/m)
$|E_{R,D}|$ = amplitude of the direct field (from the transmitter) at the receiver (mV/m)
$|E_{R,S}|$ = maximum amplitude of the scattered field (from the wind turbine) during a rotor revolution (mV/m)
m_E = ambient field modulation index
f_m = time-varying modulation shape function; $-1 \le f_m(t) \le 1$
t = time (s)

The severity of interference with the signal field is measured by the modulation index, m_E, and the nature of the interference effects is described by the modulation shape function, f_m. The envelope of $|E_R|$ represents the field of the total signal that is actually observed, and the modulation shape function represents the time dependence of the envelope of the scattered signal introduced by the blade rotation.

The perception of electromagnetic interference depends not only on the modulation of the ambient signal field but also on the degree of modulation of the signal power at the input terminals of the receiver. This involves the *receiving antenna orientation and response.* In a TV signal, for example, signal power and signal field are related as follows:

$$P_R = G_o F_A (\lambda/693\pi)^2 E_R^2 \tag{2}$$

where
P_R = signal power *input* at the receiver location (mW)
G_o = effective gain of the receiving antenna pointed at the transmitter (mW/mV^2)
F_A = azimuthal response factor of the receiving antenna, dependent on ϕ_A; $F_A \le 1$, with $F_A(0°) = 1$ and $F_A(\pm 180°) = F_{B/F}$ (mW/mW)
$F_{B/F}$ = back-to-front ratio of a directional antenna
ϕ_A = azimuthal angle from the receiving antenna beam to the signal source (rad)
λ = signal wave length = $299.8/f$ (m)
f = signal frequency (see **Appendix A** for TV channel frequencies) (MHz)

Signal power is usually expressed in *dBm* or *dB above 1 mW*, for which the definition is

$$P_R\,(dBm) = 10 \log_{10} [P_R\,(mW)] \tag{3}$$

Typical azimuthal response functions for a directional TV antenna are shown in Figure 3. Figure 3(a) presents the results of a laboratory test at one signal frequency as a polar diagram in which F_A is equal to the difference between the dB reading at a given antenna direction and

that at zero degrees. In Figure 3(b), the equivalent response in the field is compared to the laboratory or "free space" data, showing the effects of local terrain and atmospheric conditions.

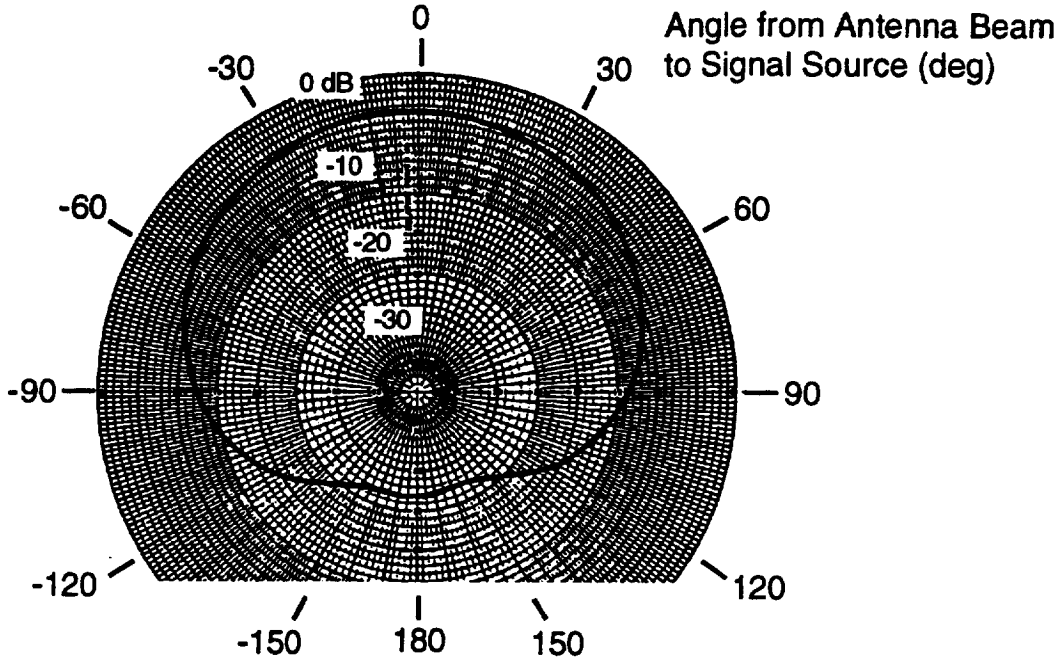

(a)

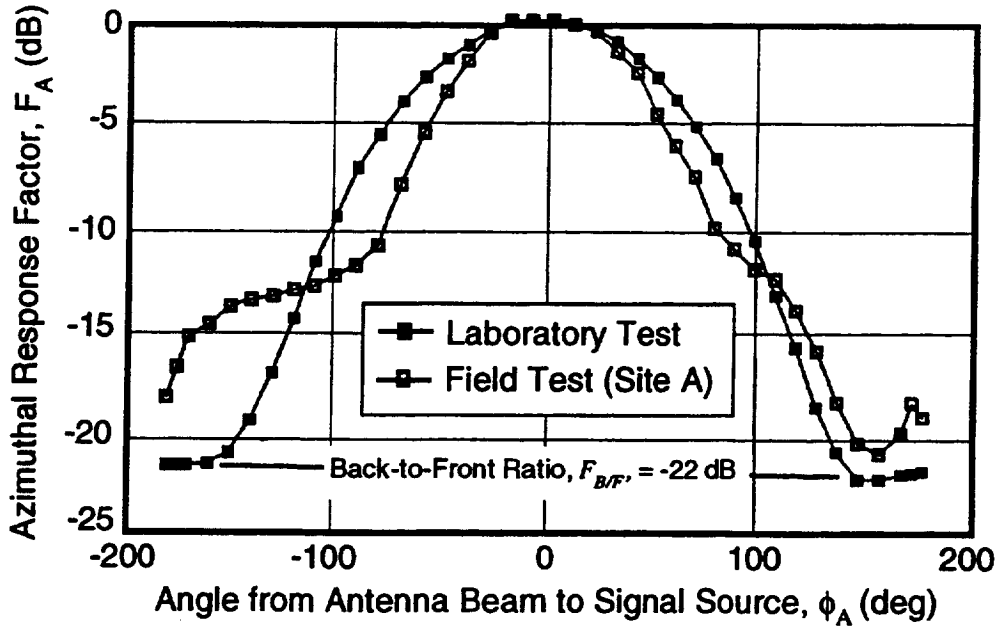

(b)

Figure 3. Typical azimuthal response factors for a directional TV antenna.
(a) Laboratory calibration at 63 MHz (Ch. 3). (b) Field response at approximately 66 MHz, compared with the laboratory calibration. [Ref. 5]

Figure 4 shows typical modulations of an audio power signal that can be caused by the addition of a secondary signal scattered by a HAWT rotor. In this case the turbine is the 2.0-MW Mod-1 machine with two steel blades rotating at 10 rpm, which produces a modulation wave form with a period of 3.0 s. In Figure 4(a), the antenna beam is pointed at the wind turbine, at an azimuth of 288 deg. The direct (desired) signal is received from the transmitter at an azimuth of 154 deg. Thus, the antenna angle for the direct signal is 134 deg, for which the response factor (Fig. 3) is -12 to -18 dB. This greatly increases the relative size of the modulation compared to the direct signal. Figure 4(b) shows that the opposite is true when the antenna is directed at the wind transmitter. Here the direct signal is received at full strength and the scattered signal is reduced by -12 to -18 dB. These two signal records illustrate how potential interference can often be avoided by the use of a properly-oriented directional antenna.

Combining Equations (1) and (2) gives

$$|P_R|_{envelope} = |P_{R,D}|\,(1 + m_R f_m)^2 \tag{3a}$$

$$m_R = \sqrt{F_{A,W}/F_{A,T}}\; m_E \tag{3b}$$

where $|P_{R,D}|$ = amplitude of direct signal power input at the receiver location (mW)
m_R = receiver input modulation index
$F_{A,W}$ = antenna response factor for a signal from the wind turbine (mW/mW)
$F_{A,T}$ = antenna response factor for a signal from the transmitter (mW/mW)

Because the maximum magnitude of f_m is always unity, the maximum and minimum departures (in dBm) from the level of the direct signal are

$$\Delta_1 = 20 \log_{10}(1 + m_R) \tag{4a}$$

$$\Delta_2 = 20 \log_{10}(1 - m_R) \tag{4b}$$

giving rise to

$$\Delta = \Delta_1 - \Delta_2 = 20 \log_{10}\left(\frac{1 + m_R}{1 - m_R}\right) \tag{4c}$$

where $\Delta = P_{R,\,max} - P_{R,\,min}$ = signal power modulation range (dBm)
$\Delta_1 = P_{R,\,max} - P_{R,\,mean}$ (dBm)
$\Delta_2 = P_{R,\,min} - P_{R,\,mean}$ (dBm)
$P_{R,\,mean} = |P_{R,D}|$ (dBm)

Figure 5 is a graphical solution of Equation (4c), from which we obtain the following empirical equation:

$$m_R = 0.0620\,\Delta\,(1 - 0.0169\,\Delta) \tag{5}$$

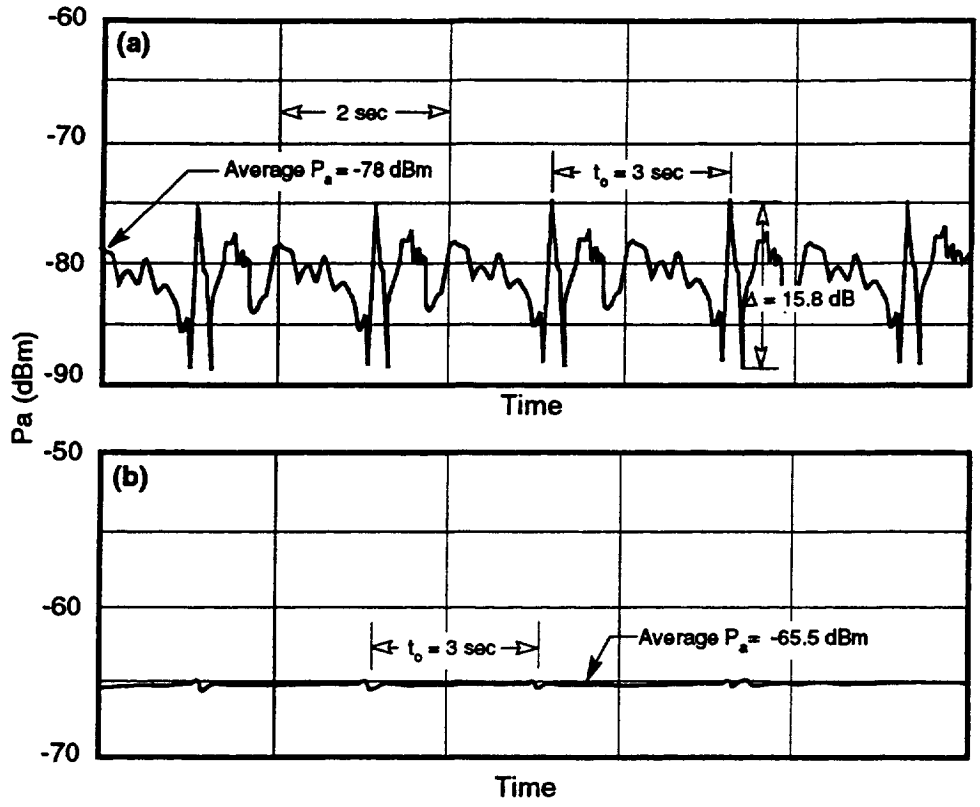

Figure 4. Typical modulation of a TV power signal by a secondary signal scattered by an operating wind turbine. (a) Antenna pointed at the transmitter. (b) Antenna pointed at the wind turbine. The turbine is the two-bladed 2.0-MW Mod-1 HAWT and the signal is on Channel 3. Modulation wave frequency is twice the turbine rotor speed of 10 rpm [Ref. 5].

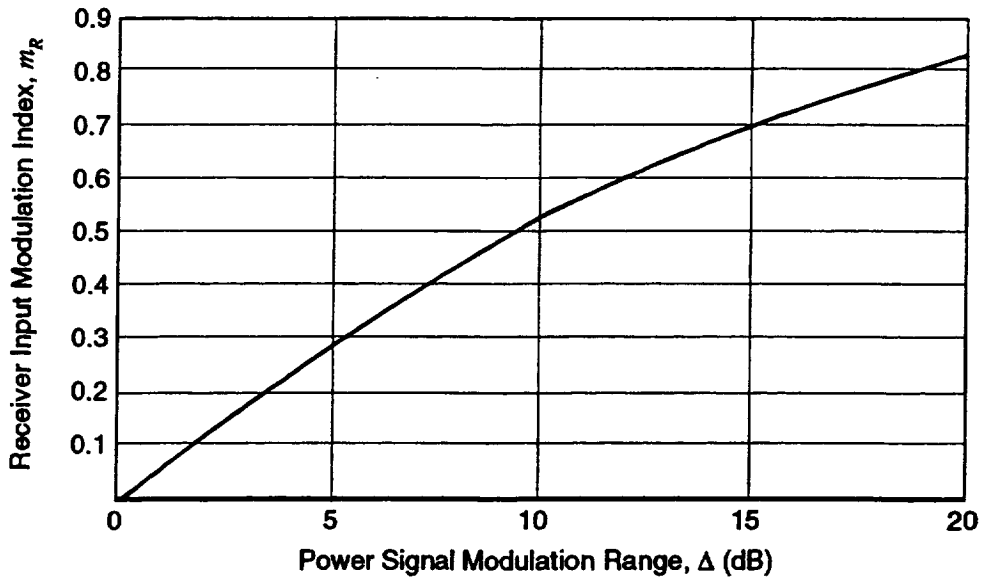

Figure 5. Receiver modulation index versus the power signal modulation range.

Observed Signal Scatter Ratios

The strength of the scattered signal field at a receiver location caused by a wind turbine can be conveniently expressed as a *signal scatter ratio*, which is the ratio of the amplitude of the scattered signal field *at the receiver* to the direct signal field *at the turbine*, or

$$Z = \frac{|E_{R,S}|}{|E_{WT,D}|} \tag{6}$$

where Z = signal scatter ratio
$|E_{WT,D}|$ = amplitude of the direct field at the wind turbine (mV/m)

The ratio Z is a characteristic of the turbine and its location relative to the transmitter and receiver, and it is independent of the receiver antenna response or the ambient signal fields at either the receiver or turbine locations. The signal scatter ratio can be used to predict the receiver input modulation index using Equations (1b) and (3b), as follows:

$$m_R = Z\sqrt{\frac{F_{A,W}}{F_{A,T}}}\,\frac{|E_{WT,D}|}{|E_{R,D}|} \tag{7}$$

Equation (7) shows clearly that EMI potential depends on the combination of turbine and site characteristics (Z), relative antenna characteristics ($F_{A,W}/F_{A,T}$), and relative direct field strengths ($|E_{WT,D}|/|E_{R,D}|$).

The signal scatter ratio actually observed during a test can be determined from a record of signal power versus time, like that shown in Figure 9-4(a). Data reduction equations, derived from Equations (2), (4), (5), and (6), are

$$Z_O = \frac{|E_{R,S}|_O}{|E_{WT,D}|} = \frac{m_R(\Delta)}{\sqrt{F_{A,W}}}\,\frac{\sqrt{P_{R,mean}}}{\sqrt{|P_{WT,D}|}} \tag{8a}$$

$$P_{R,mean} = \frac{P_{R,\max}}{(1+m_R)^2} \tag{8b}$$

$$F_{A,W} = \frac{[P_{R,mean}]_W}{P_{R,mean}} \tag{8c}$$

where Z_O = observed signal scatter ratio
$|E_{R,S}|_O$ = observed amplitude of the scattered signal at the receiver (mV/m)
$|P_{WT,D}|$ = amplitude of the direct signal power at the wind turbine rotor (mW)
$[P_{R,mean}]_W$ = average signal power with the antenna beamed at the wind turbine (mW)

The following calculations of scatter ratios for the signals in Figure 4 will illustrate the use of Equations (8):

From measurements of the power of the direct signal at the wind turbine site, $P_{WT,\,D}$ = -27.0 dB. Let $Z_O = Z_W$ when the antenna is aimed at the wind turbine and $Z_O = Z_T$ when it is aimed at the transmitter. Ideally, the ratios Z_W and Z_T will be equal.

Case 9: Antenna aimed at the wind turbine (Case numbers refer to the listing in Appendix B)

From Figure 4(a),

$$\Delta = P_{R,\,max} - P_{R,\,min} = -74.5 - (-89.5) = 15.0 \text{ dB}$$

$$m_R = 0.0620\,\Delta(1 - 0.0169\,\Delta) = 0.695$$

$$P_{R,\,mean} = P_{R,\,max}/(1 + m_R)^2 = 10\log_{10}[10^{-7.45}/(1.695)^2] = -79.1 \text{ dB}$$

$$F_{A,\,W} = [P_{R,\,mean}]_W / P_{R,\,mean} = -79.1 - (-79.1) = 0 \text{ dB}$$

$$Z_W = 10\log_{10}(m_R) + 0.5(P_{R,\,mean} - F_{A,\,W} - P_{WT,\,D}) = -27.6 \text{ dB} = 0.0017$$

Case 10: Antenna aimed at the transmitter

From Figure 4(b),

$$\Delta = -64.7 - (-65.2) = 0.5 \text{ dB}$$

$$m_R = 0.0620 \times 0.5(1 - 0.0169 \times 0.5) = 0.031$$

$$P_{R,\,mean} = 10\log_{10}[10^{-6.47}/(1.031)^2] = -65.0 \text{ dB}$$

$$F_{A,\,W} = -79.1 - (-65.0) = -14.1 \text{ dB}$$

$$Z_T = 10\log_{10}(0.031) + 0.5[-65.0 - (-14.1) - (-27.0)] = -27.1 \text{ dB} = 0.0020 \approx Z_W$$

In these two cases, the turbine scatters about 0.2 percent of its incident field onto the receiver.

Idealized Signal Scatter Ratios

It has been found that the main scattering characteristics of a rotating HAWT blade can be adequately analyzed with the help of an idealized model consisting of a rotating flat plate [*e.g.*, see Ref. 5]. To simplify the model and maximize the strength of the scattered signal, the blades of the wind turbine are assumed to be positioned for optimum reflection (or shadowing) of the signal from the transmitter, all elevations (transmitter, wind turbine, and receiver) are assumed equal, and earth reflection effects are neglected. Under these conditions, an idealized signal scatter ratio can be defined as follows:

$$Z_I = \frac{|E_{R,S}|_I}{|E_{WT,D}|} = \eta_S \frac{B_E A_P}{\lambda \zeta} \cos(k \phi_S) \tag{9a}$$

$$k = \begin{cases} 0.5, & -0.8\pi \le \phi_S \le 0.8\pi \quad (\textit{Backward Zone}) \\ 2.0, & 0.8\pi \le \phi_S \le 1.2\pi \quad (\textit{Forward Zone}) \end{cases} \tag{9b}$$

where
Z_I = idealized signal scatter ratio
$|E_{R,S}|_I$ = idealized amplitude of the scattered signal field at the receiver (mV/m)
η_S = signal scattering efficiency of a blade compared to a flat metallic plate
B_E = effective number of blades, $\le B$ = actual number of blades
A_P = planform area of one blade (m^2)
λ = wave length of the direct signal (m)
ζ = distance from the receiver to the wind turbine (m)
ϕ_S = azimuthal scatter angle, from transmitter to wind turbine to receiver (rad)

Signal Scattering Efficiency of a HAWT Blade

Laboratory tests of the signal-scattering efficiency of scale-model HAWT blades [e.g. Refs. 3 and 4], using microwave signals in an *anechoic chamber*, have identified the relative effects of *airfoil contour*, *material*, and *total twist*. The results of these experiments are summarized in Figure 6, and they lead to the following empirical equations:

$$\eta_{S,H} = \eta_A \eta_M \exp(-2.30\,\Delta\beta) \tag{9c}$$

$$\eta_A = 0.80 \tag{9d}$$

$$\eta_M = \begin{cases} 1.00 & \textit{for metallic blades} \\ 0.41 & \textit{for non-metallic blades} \end{cases} \tag{9e}$$

where
$\eta_{S,H}$ = signal scattering efficiency of a HAWT blade
η_A = airfoil contour factor
η_M = material factor
$\Delta\beta$ = total blade twist from root to tip (rad)

Lightning protection in the form of spanwise metallic strips may increase the scattering efficiency of a non-metallic blade almost to that of a completely metallic blade [Ref. 4].

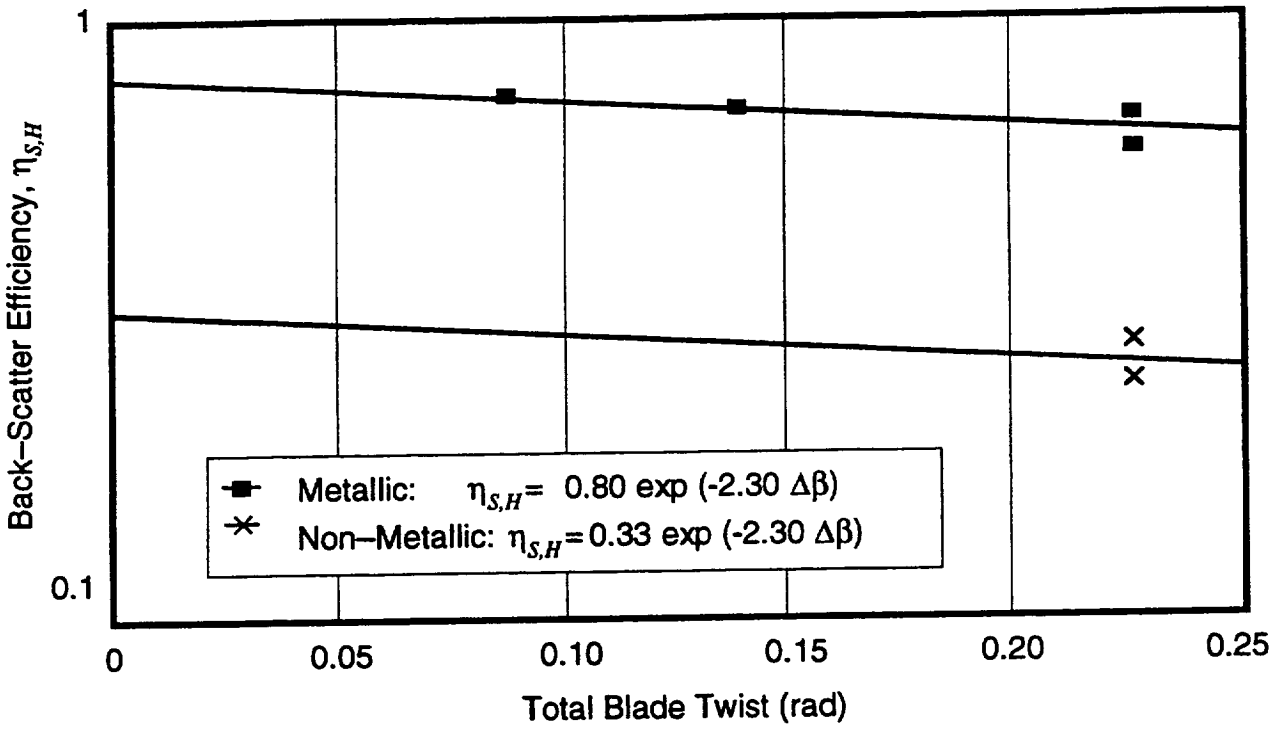

Figure 6. Signal scattering efficiency of scale-model HAWT blades compared to flat, metal plates. [data from Refs. 3 and 4]

Signal Scattering Efficiency of a Darrieus VAWT Blade

During television interference tests around the curve-bladed DOE/Sandia 17-m Darrieus VAWT (Fig. 1(b)), it was observed that the strength of the scattered field was relatively independent of the carrier wave length, λ [Ref. 6]. Referring to Equation (9a), this suggests that the scattering efficiency, η_S, must be proportional to λ for a Darrieus rotor. This was confirmed by tests in which the receiver was directly between the transmitter and the VAWT. For this test configuration, ϕ_S equals zero. B_E equals one, since maximum scatter occurs when one blade is directly between the VAWT axis and the receiver and this places the other blade in its shadow and in the shadow of the central column of the rotor. Combining Equations (8a) and (9a), the observed signal scattering efficiency, $\eta_{S,O}$, for this arrangement is

$$\eta_{S,O} = \frac{Z_O \lambda \zeta}{A_P}$$

Figure 7 shows the observed scattering efficiency of the 17-m Darrieus VAWT blade as a linear function of the wave length normalized by the blade length of 24.1 m, which leads to

$$\eta_{S,V} = \eta_A \eta_M \lambda/L \tag{9f}$$

where $\eta_{S,V}$ = signal scattering efficiency of a Darrieus VAWT blade

The airfoil and material factors for a VAWT blade are assumed to be the same as those for a HAWT blade, as given in Equations (9d) and (9e). Equation (12) should be considered to be preliminary until verified by scattering tests on Darrieus blades of other lengths.

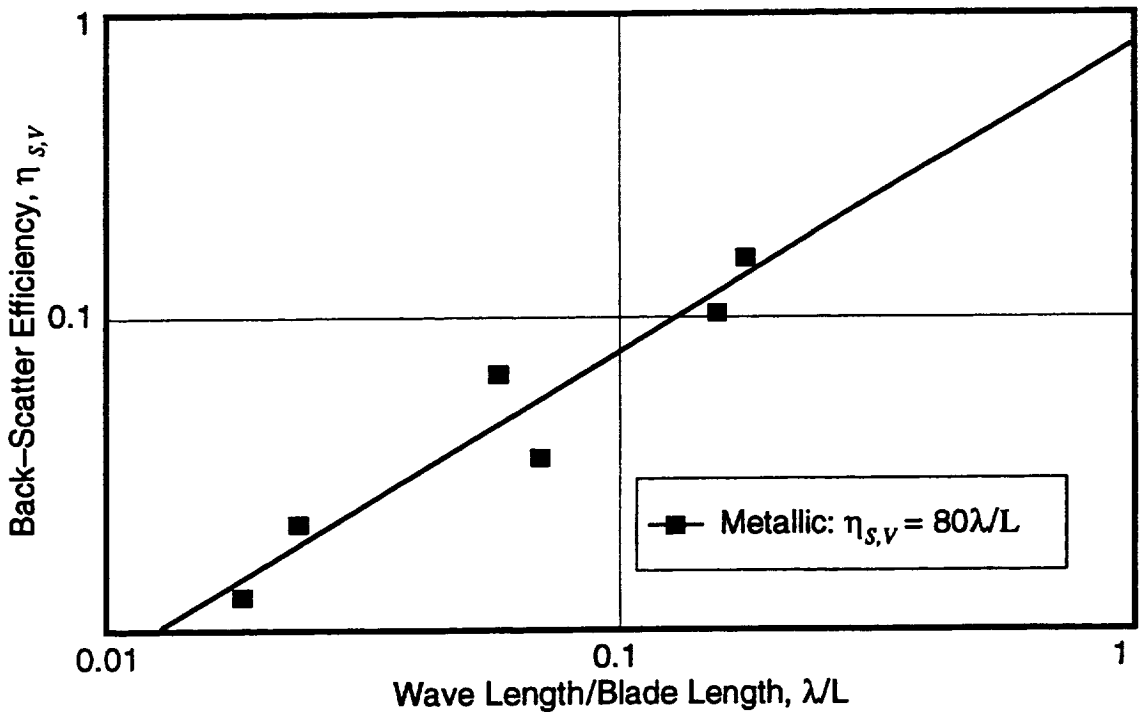

Figure 7. Signal scattering efficiency of a Darrieus VAWT blade compared to a flat metal plate of the same planform area. [data: Ref. 6]

Effective Number of Blades

The parameter B_E accounts for the fact that the axes of multiple blades on a wind turbine rotor may not be collinear, so that when one blade is in its maximum scattering position the other (or others) may not be. For an idealized, two-bladed HAWT rotor with coning (i.e., blades tilted downwind to reduce bending loads), if blade 1 is horizontal and positioned for maximum scattering, the aximuthal position of blade 2 will differ from that of blade 1 by twice the coning angle. For this configuration, it can be shown that

$$B_E = 1 + sinc\left\{\frac{2\pi l}{\lambda}\sin(2\theta)\cos(k\phi_S)\right\} \le B \tag{9f}$$

where $sinc\{\ \} = |\sin\{\ \} / \{\ \}|$

θ = coning angle between the blade axis and the plane of revolution (rad)

It can be shown that Equation (9f) also applies to an idealized three-bladed rotor. When calculating the idealized signal scatter ratio for a HAWT, it is necessary to place an upper limit on B_E that may be less than B, to prevent the scattered signal from exceeding the direct signal at distances from the turbine greater than the rotor radius. Referring again to Equation (9a),

$$B_E \le B_{E,\max} = \lambda R/A_P \qquad \textit{for HAWT rotors} \tag{9g}$$

Equation (9g) can be applied to VAWT rotors by assuming that coning angles are determined by the angles between airfoil sections at the rotor equator. Thus, the coning angle is zero for a two-bladed VAWT and 60 deg for a VAWT with three blades. In the infrequent case when the receiver is directly between the transmitter and a two-bladed VAWT, only one blade is effective.

Multiple Wind Turbines

Measurements in the vicinity of three MOD-2 wind turbines [Ref. 10] indicate that TVI effects are enhanced when several turbines operate in synchronism (i.e.with blades parallel). The amplitude of the interference pulses produced by two synchronized turbines is about twice that for a single wind turbine. For a large number of units, interferences may add randomly, but this is yet to be verified. A practical approach to analyzing the scattering of signals by a wind power plant composed of a large number of turbines is to divide the plant into clusters and use the following two assumptions about cumulative scattering: (1) The turbines within a cluster operate in synchronism, so that the idealized cluster scatter ratio is the sum of the individual ratios within the cluster, and (2) clusters are not in synchronism, so the idealized plant scatter ratio is the root-sum-square (RSS) of the cluster ratios. On the basis of these assumptions,

$$Z_{I,C} = \frac{|E_{R,S}|}{|E_{C,D}|} = \sum_{j=1}^{N} Z_{I,j} \tag{9h}$$

$$Z_{I,PS} = \frac{|E_{R,S}|}{|E_{PS,D}|} = \sqrt{\sum_{i=1}^{M}\left[Z_{I,C}^2\right]_i} \tag{9i}$$

$$|E_{C,D}| = \frac{1}{N}\sum_{j=1}^{N}|E_{WT,D}|_j \qquad |E_{PS,D}| = \frac{1}{M}\sum_{i=1}^{M}|E_{C,D}|_i \tag{9j}$$

where $Z_{I,C}$ = idealized cluster scatter ratio

$Z_{I,PS}$ = idealized power station scatter ratio

N, M = number of wind turbines in a cluster and number of clusters, respectively

$|E_{C,D}|, |E_{PS,D}|$ = average amplitudes of the direct signals incident on a cluster and on the power station, respectively (mV/m)

Comparison of Observed and Idealized Signal Scatter Ratios

For the conditions of a given field test, Equations (8) can be used to calculate the observed scatter ratio, while an idealized scatter ratio is determined for that test using Equations (9). By comparing observed and idealized scatter ratios for a variety of wind turbines and field conditions, we can estimate the probability that signal interference will exceed the idealized value by a given amount. This has been done for the 75 field test cases listed in Table 1. Data for calculating the observed scatter ratios are tabulated in Appendix B for these cases, and Appendix C contains a tabulation of idealized scatter ratios.

Table 1.
TVI Cases Analyzed for Observed vs Idealized Scatter Ratios
(Data in Appendices B and C)

Wind turbine	No. of units	Scatter zone	No. of cases	Wave lengths (m)	WT-Receiver distances (m)	Source of data
Mod-1 HAWT	1	Backward	15	1.6 - 5.0	1041 - 2745	[Ref. 1]
"	"	Forward	5	1.5 - 3.7	"	"
Mod-2 HAWT	1	Backward	4	1.6 - 3.4	1603 - 6100	[Ref. 2]
"	"	Forward	1	0.6	1445	"
"	2	Backward	1	3.4	6254	"
"	2,3	Forward	4	0.5 - 1.4	1354 - 1717	"
17-m VAWT	1	Backward	33	0.4 - 4.2	32 - 133	[Ref. 3]
"	"	Forward	12	"	27 - 31	"
		Total:	75			

Backward Scatter Zone

Figure 8 presents a comparison of observed and idealized signal scatter ratios (in dB) for 53 cases in which the receiver was located in the backward scatter zone. Correlation is approximately the same for HAWT and VAWT tests, with most of the observed scatter ratios lying within +3 to -6 dB of the applicable idealized scatter ratio. Deviations can be attributed to rotor blades out of position for maximum scattering, ground reflection effects, atmospheric effects, and weak signals that make measurement of modulation difficult.

Forward Scatter Zone

In Figure 9, signal scatter data for receivers in the forward zone are shown for a smaller number of tests (22 cases). In the forward zone an observed scatter ratio is generally between +4 and -3 dB of its idealized ratio. The relatively large VAWT scatter ratios are caused by small distances between the turbine and the receiver (less than 2 rotor diameters for these tests). On the other hand, the larger HAWT ratios are produced by the combined effects of several large-scale rotors operating in synchronism.

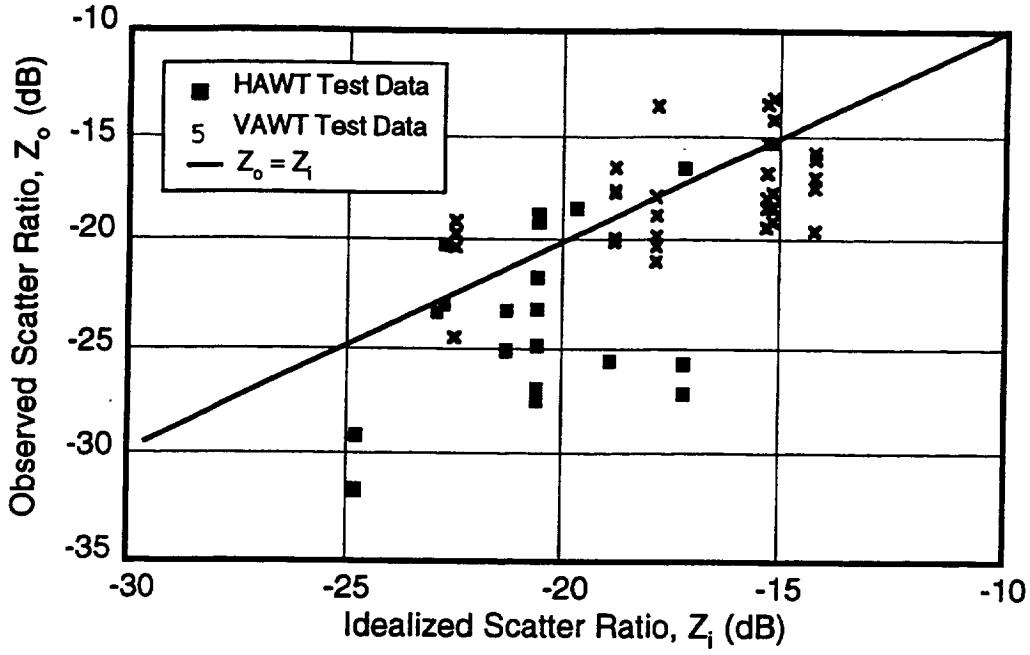

Figure 8. Comparison of observed and idealized signal scatter ratios for receivers in the backward-scatter zone.

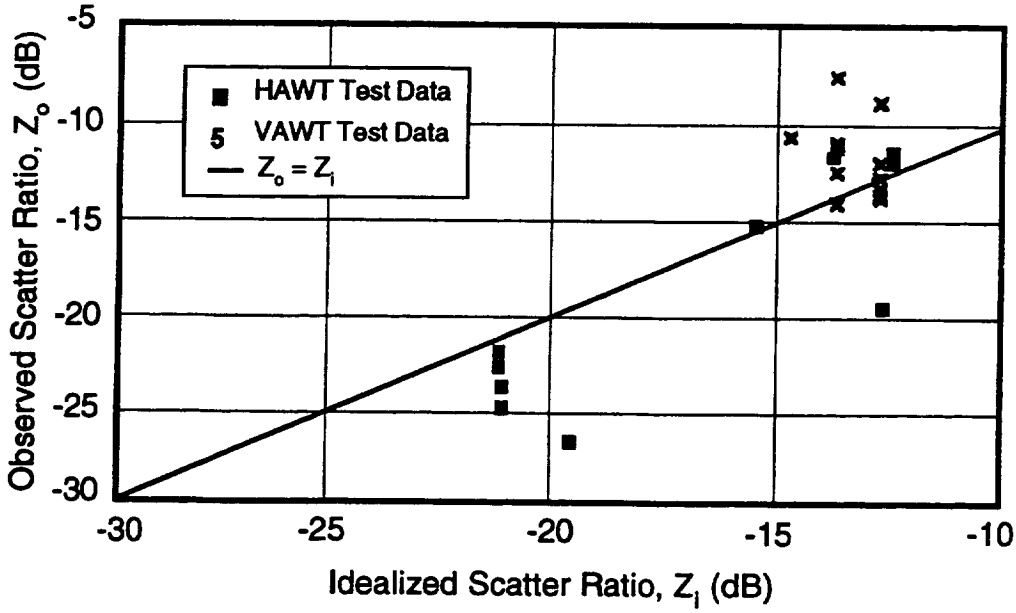

Figure 9. Comparison of observed and idealized signal scatter ratios for receivers in the forward-scatter zone.

Multiple Wind Turbines

The assumption that signal scatter ratios are linearly additive for a small cluster of wind turbines can be evaluated by examining Figure 10. TV signals scattered by two and three large-scale Mod-2 HAWTs operating simultaneously were observed to be as strong or stronger than predicted by the sum of the idealized scattered signals from each turbine.

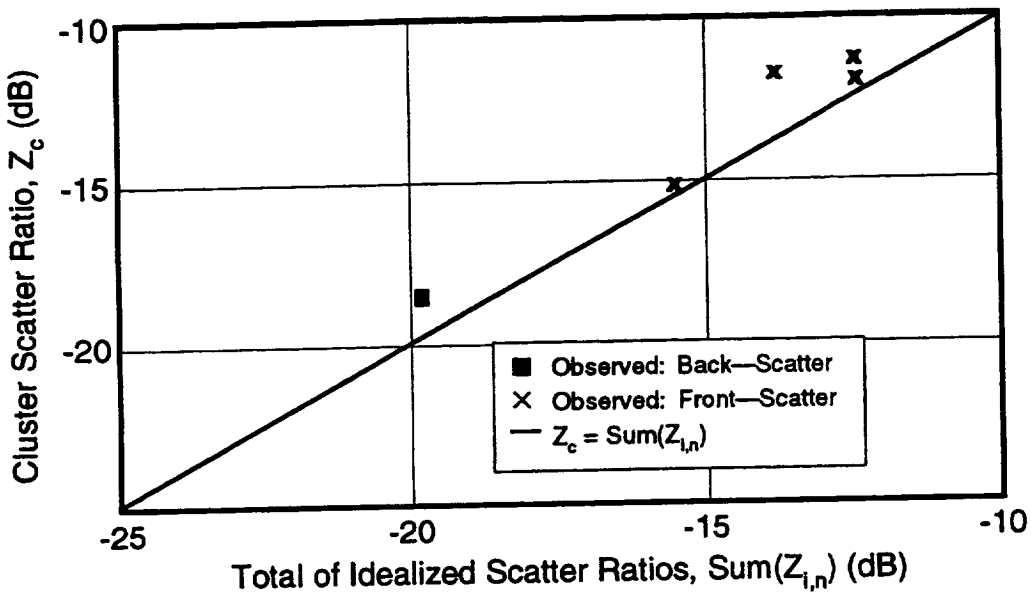

Figure 10. Comparison of observed and idealized signal scatter ratios for two and three Mod-2 HAWTs operating simultaneously. Based on test data from Reference 3.

Probability Analysis of Deviations Between Observed and Idealized Scatter Ratios

Figures 8 through 10 show that the idealized scattering model expressed in Equations (9) represents the general signal interference behavior of a variety of wind turbines under a range of field conditions. However, observed scatter ratios often deviate significantly from idealized ratios, which is to be expected since the simplified model treats several variable parameters as constants (e.g. rotor positions and relative elevations). We can estimate the effect of field conditions that differ from the assumptions in the scattering model by a statistical comparison of the results of the cases in Table 1.

A useful predictive parameter is the estimated probability that the observed signal scatter ratio will exceed the idealized ratio by a given amount, or

$$Y(\Delta Z_O > \Delta Z) = Y_E(\Delta Z) \tag{10a}$$

$$\Delta Z_O = Z_O - Z_I \tag{10b}$$

where $Y(\ )$ = probability of ( ); $0 \le Y \le 1$
$Y_E(\ )$ = probability of exceeding ( )
ΔZ_O, ΔZ = observed and selected deviations in the signal scatter ratio (dB)

Figure 11 shows the probability of exceedance as a function of the deviations for the 75 cases in Table 1. A linear fit to the central portion of this distribution is

$$Y_E(\Delta Z) = 0.39 - 0.11\,\Delta Z \qquad -5.5 \le \Delta Z \le 3.5 \tag{11a}$$

from which

$$Z = Z_I + 3.5 - 9.0 Y_E \tag{11b}$$

where all quantities are in dB units. In ratio form,

$$Z = F_E Z_I \tag{11c}$$

$$F_E = 10^{(0.35 - 0.90 Y_E)} \tag{11d}$$

where F_E = empirical exceedance factor

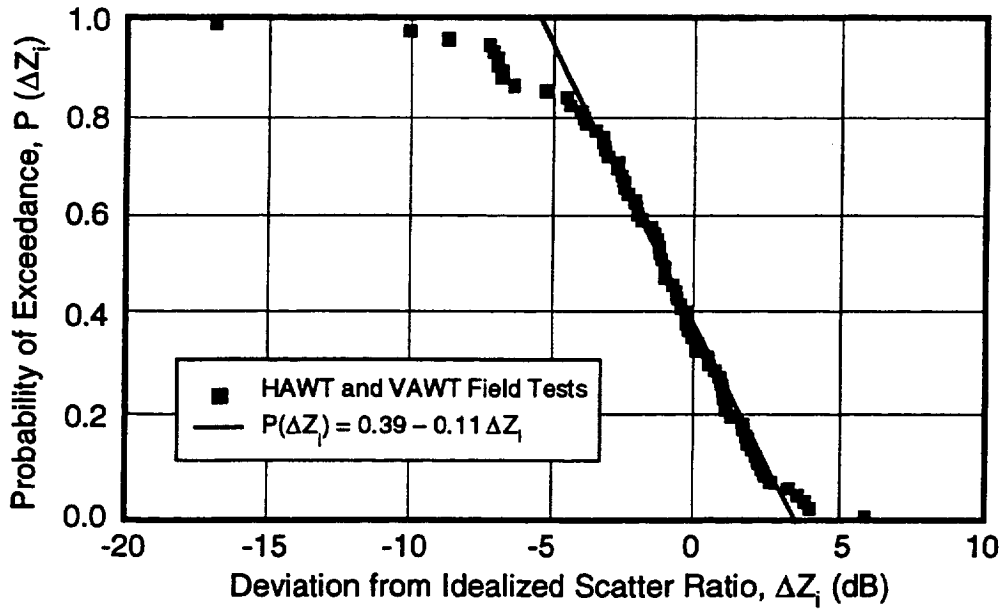

Figure 11. Probability analysis of deviations between observed and idealized signal scatter ratios. Data points are the cases listed in Table 1 and tabulated in Appendices B and C.

Interference Zone Around a Wind Power Station

The interference zone around a wind turbine or group of turbines is defined as the region within which the receiver modulation index, m_R, exceeds a long-term tolerance value, m_L, when the maximum scattered signal is being directed toward the receiver [Ref. 13]. The boundary of the interference zone is not clearly defined, since the contributing factors of signal strength, amplitude of modulation by the turbine blades, and tolerance of video distortion can all change with time. What will be presented here is a sample application of the equations developed in earlier sections, in which a boundary line is drawn around a hypothetical wind power station at a location where the modulation index is equal to 0.015. This is a typical maximum value of the index for long-term tolerance.

General Equation for Defining the Interference Zone Boundary

For this sample case, the wind power station is assumed to be composed of M clusters of N identical HAWTs at the same elevation as the transmitter and the receiver. The scatter ratios from the turbines within a cluster are assumed to be linerly additive, while cluster scatter ratios add in a random fashion. Two additional simplifying assumptions are that the receiving antenna is aimed directly at the receiver (i.e. $F_{A,T} = 1$), and the direct signal strengths at all of the turbine clusters are equal. With these assumptions, Equations (7), (9h), (9i), and (11c) can be combined to give

$$m_{R,PS} = \sqrt{\sum_{i=1}^{M} \left[Z_C \sqrt{F_{A,W}} \frac{|E_{C,D}|}{|E_{R,D}|} \right]_i^2} = N F_E \frac{|E_{PS,D}|}{|E_{R,D}|} \sqrt{\sum_{i=1}^{M} \left[F_{A,W} Z_I^2 \right]_i} \tag{12}$$

where $m_{R,PS}$ = index of total modulation caused by all turbines in the wind power station

Maximizing the effective number of blades in accordance with Equation (9g), the idealized signal scatter ratio in Equation (9a) becomes

$$Z_I = \eta_S \left(\frac{\lambda R}{A_P} \right) \frac{A_P}{\lambda \zeta} \cos(k \phi_S) = \frac{\eta_S}{2} \frac{D}{\zeta} \cos(k \phi_S) \tag{13a}$$

$$k = \begin{cases} 0.5, & -0.8\pi \le \phi_S \le 0.8\pi \quad (\textit{Backward Zone}) \\ 2.0, & 0.8\pi \le \phi_S \le 1.2\pi \quad (\textit{Forward Zone}) \end{cases} \tag{13b}$$

where the parameters ζ, ϕ_S, and k are evaluated for each cluster. Combining Equations (12) and (13) and solving for the distance from the center of the power station, the following equation is obtained which defines the boundary of the interference zone in polar coordinates:

$$\zeta_B(\phi_B) = \frac{\eta_S D N F_E}{2 m_{R,PS}} \frac{|E_{PS,D}|}{|E_{R,D}|} \sqrt{\sum_{i=1}^{M} \left[F_{A,W} \left(\zeta_B / \zeta \right)^2 \cos^2(k \phi_S) \right]_i} \tag{14}$$

where ς_B = radial distance from the center of the power station to a given point on the interference zone boundary (m)

ϕ_B = azimuthal angle from the transmitter to the center of the power station to the same boundary point (deg)

To solve Equation (14), the coordinates ς_i and $\phi_{S,i}$ for each cluster are first expressed in terms of the coordinates ζ_B and ϕ_B. A value of ϕ_B is then selected, and a corresponding value of ζ_B is determined by trial and error that will make the two sides of Equation (14) equal.

Sample Wind Power Station Configuration

Figure 12 is a schematic plan of the sample power station, which is composed of 60 HAWTs divided into 10 clusters of 6 turbines each. The turbines are 40 m in diameter and are arranged in three north-south rows, with spacings of 240 m (6*D*) east-west and 120 m (3*D*) north-south. The station boundary is assumed to be 3*D* from the outer turbines, which gives a total station size of 720 m x 2,520 m. The transmitter is located directly north of the station.

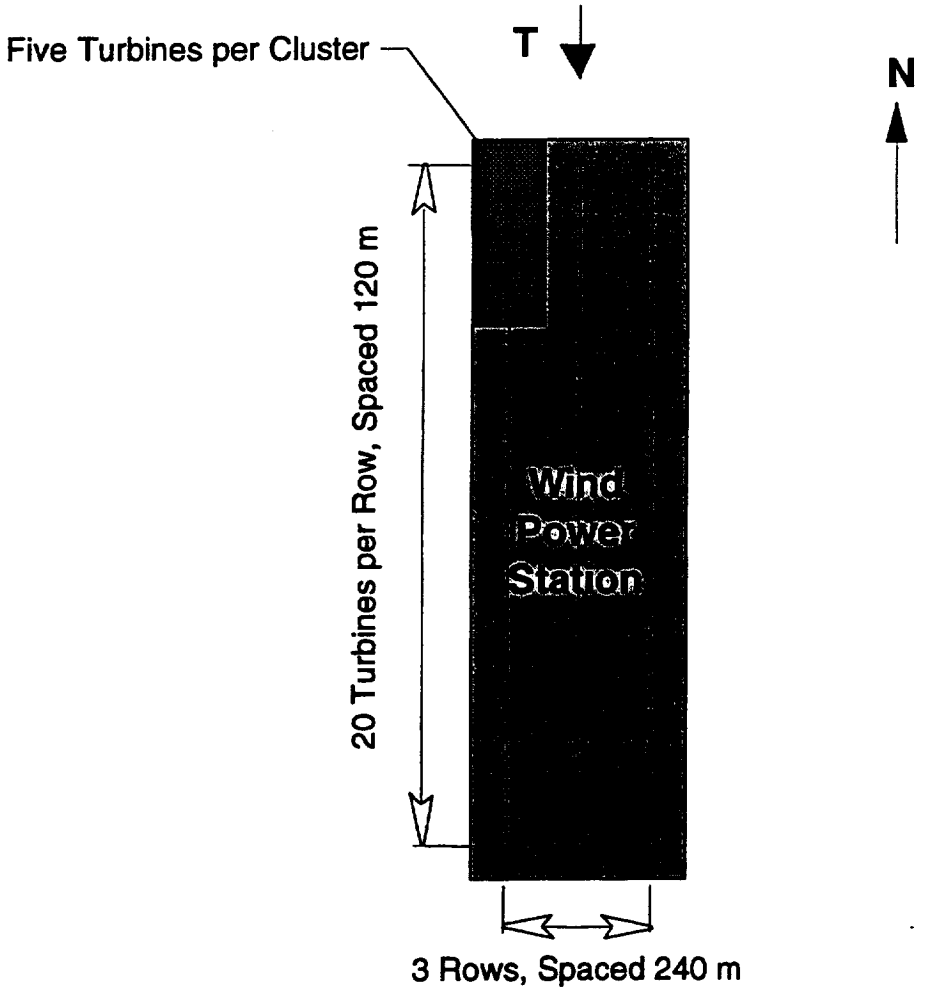

Figure 12. Schematic plan view of the sample wind power station.

The parameters in Equation (14) are evaluated as follows for this sample station:

$$
\begin{aligned}
D &= 40 \text{ m} \\
M &= 10 \\
N &= 6 \\
\eta_S &= 0.50 \\
F_E &= 2.02 \quad \text{(i.e. } Y_E = 0.05\text{)} \\
m_{R,PS} &= 0.15 \\
|E_{PS,D}| &= |E_{R,D}| \\
F_{A,W} &= F_{B/F}\,[1 + \cos(\phi_S)]/2 \quad \text{(dB)} \\
F_{B/F} &= 0, -5, -10, -15, \text{ and } -20 \text{ dB}
\end{aligned}
$$

With these parameters, Equation (14) becomes

$$\zeta_B(\phi_B) = 808 \sqrt{\sum_{i=1}^{10} \left[10^{F_{B/F}[1 + \cos(\phi_S)]/20} \, (\zeta_B/\zeta)^2 \cos^2(k\phi_S) \right]_i} \quad (m) \qquad (15)$$

Figure 13 shows the boundaries of the TV interference zones with a modulation index of 0.15 for various values of the back-to-front ratio of the receiving antenna. Examination of Figure 13 shows that the directionality of the receiving antenna is important in the broad backward-scatter zone to the north of the station, but not significant in the narrow forward-scatter zone to the south.

Conclusions

Equations have been developed with which the extent of potential interference with TV signals by the moving blades of a wind turbine or group of wind turbines can be estimated. These equations include the effects of parameters that significantly influence TV signal modulation, as determined by tests in the laboratory and in the field. These parameters include the relative locations of the transmitter, wind turbine(s), and receiver; size, material, and shape of the wind turbine blades; numbers and spacing of multiple wind turbines; directionality of the receiving antenna; frequency and power of the direct signal; and reflectivity of the terrain between the turbines and the receiver. The equations also include a factor that permits the analyst of incorporate a probability of exceedance into the interference estimates.

The equations presented are based on available test data and applicable models of electromagnetic interference, but field test data from multiple wind turbines are limited to measurements around three megawatt-scale HAWTs with metal blades. Measurements of the intensity of scattered signals around wind power stations containing large numbers of turbines of various sizes with metallic and non-metallic blades are needed to validate the equations presented for estimating the size of the potential TV interference zone around such installations.

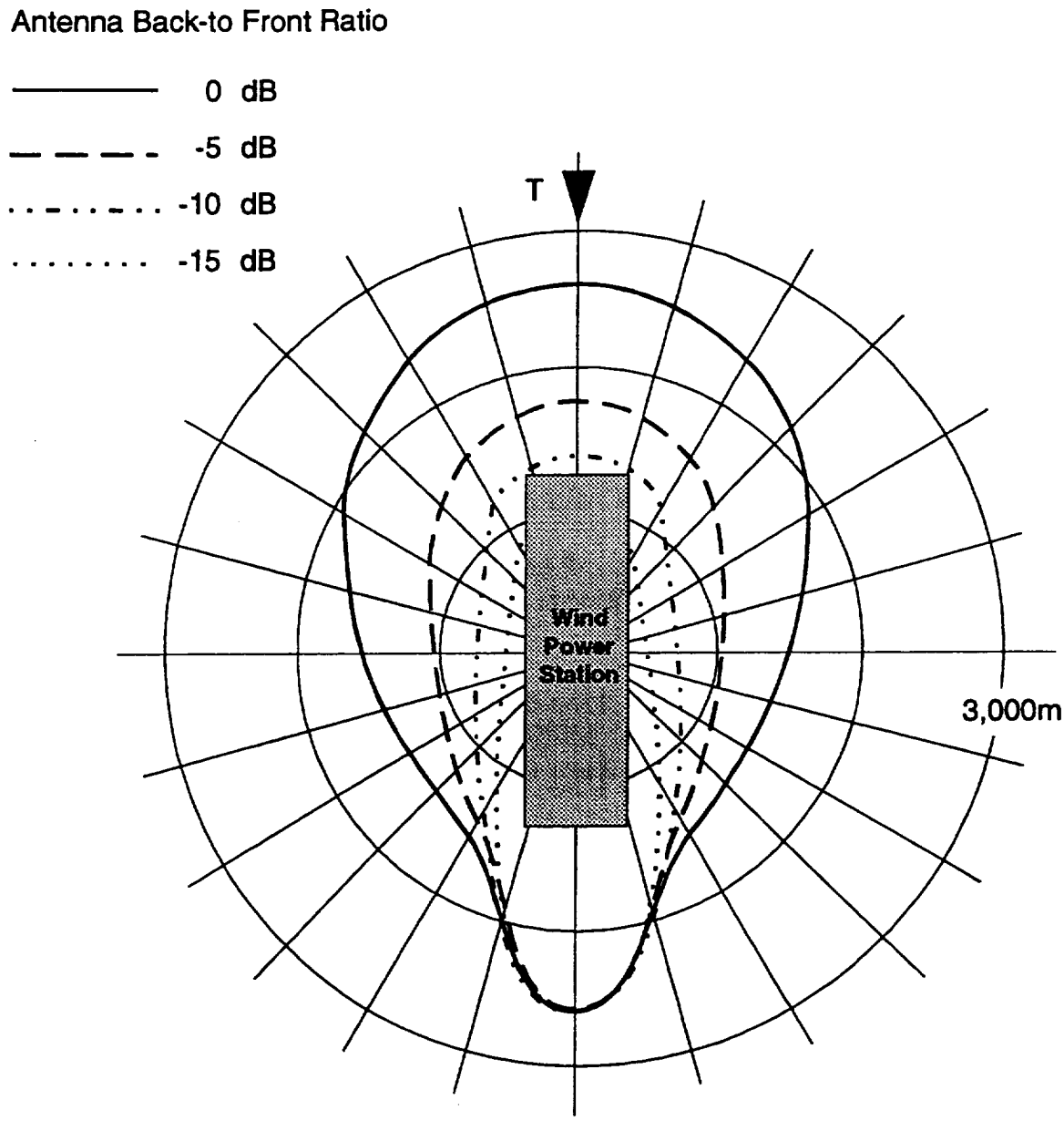

Figure 13. TV interference zones around the sample wind power station in Figure 12, for various values of the antenna back-to-front ratio. The modulation index at the zone boundaries is 0.15.

References

1. Senior, T. B. A.; Sengupta, D. L.; and Ferris, J. E.: TV and FM Interference by Windmills. Univ. of Michigan Radiation Lab. Final Report No. 014438-1-F, 1977.

2. Sengupta, D. L., and Senior, T. B. A.: TV and FM Interference by Windmills. Final Report DOE/TIC-11348, U.S. Dept. of Energy, 1977.

3. Sengupta, D. L., and Senior, T. B. A.: Electromagnetic Interference by Wind Turbine Generators. TID-28828, Contract No. EY-76-02-184, U.S. Dept. of Energy, 1978.

4. Sengupta, D. L., and Senior, T. B. A.: Electromagnetic Interference to Television Reception Caused by Horizontal Axis Windmills. Proc. IEEE, Vol. 67, No. 8, 1979, pp. 1133-1142.

5. Sengupta, D. L., and Senior, T. B. A.: Wind Turbine Generator Interference to Electromagnetic Systems. DOE/ET/20234-T1, U.S. Dept. of Energy, 1979.

6. Sengupta, D. L., and Senior, T. B. A.: Wind Turbine Interference to Television Reception. Univ. of Michigan Radiation Lab. Final Report No. 014438-4-F, 1980.

7. Sengupta, D. L.; Senior, T. B. A.; and Ferris, J. E.: Television Interference Tests on Block Island, RI. Tech. Report No. 3, Contract EY-76-S-02-2846, A004, U.S. Dept. of Energy, 1980.

8. Sengupta, D. L.; Senior, T. B. A.; and Ferris, J. E.: Measurements of Interference to Television Reception Caused by the MOD-1 Turbine at Boone, NC. Tech. Report No. 1, Contract DE-SERI-XH-0-9263-1, Solar Energy Research Institute, 1981.

9. Sengupta, D. L.; Senior, T. B. A.; and Ferris, J. E.: Measurements of Television Interference Caused by a Vertical Axis Wind Machine. SERI/STR-215-1881, Solar Energy Research Institute, 1981.

10. Sengupta, D. L.; Senior, T. B. A.; and Ferris, J. E.: Television Interference Measurements Near the MOD-2 WT Array at Goodnoe Hills, Washington. SERI/STR-211-2086, Solar Energy Research Institute, 1983.

11. Sengupta, D. L.; Senior, T. B. A.; and Ferris, J. E.: Study of Television Interference by Small Wind Turbines. SERI/STR-215-1880, Solar Energy Research Institute, 1983.

12. Senior, T. B. A., and Sengupta, D. L.: Large Wind Turbine Handbook: Television Interference Assessment. SERI/STR-215-1879, Solar Energy Research Institute, 1983.

13. Sengupta, D. L., and Ferris, J. E.: Assessment of Electromagnetic Interference Effects of the Ellenville Windfarm. Univ. of Michigan Radiation Lab. Final Report No. 388629-1-F, 1983.

Appendix A - Television Channel Center Frequencies

Channel number	Video signal (MHz)	Audio signal (MHz)	Channel number	Video signal (MHz)	Audio signal (MHz)
2	55.25	59.75	30	567.25	571.75
3	61.25	65.75	31	573.25	577.75
4	67.25	71.75	32	579.25	583.75
5	77.25	81.75	33	585.25	589.75
6	83.25	87.75	34	591.25	595.75
7	175.25	179.75	35	587.25	601.75
8	181.25	185.75	36	603.25	607.75
9	187.25	191.75	37	609.25	613.75
10	193.25	197.75	38	615.25	619.75
11	199.25	203.75	39	621.25	625.75
12	205.25	209.75	40	627.25	631.75
13	211.25	215.75	41	633.25	637.75
14	471.25	475.75	42	639.25	643.75
15	477.25	481.75	43	645.25	649.75
16	483.25	487.75	44	651.25	655.75
17	488.25	493.75	45	657.25	661.75
18	495.25	499.75	46	663.25	667.75
19	501.25	505.75	47	669.25	673.75
20	507.25	511.75	48	675.25	679.75
21	513.25	517.75	49	681.25	685.75
22	519.25	523.75	50	687.25	691.75
23	525.25	529.75	51	693.25	697.75
24	531.25	535.75	52	699.25	703.75
25	537.25	541.75	53	705.25	709.75
26	543.25	547.75	54	711.25	715.75
27	549.25	553.75	55	717.25	721.75
28	555.25	559.75	56	723.25	727.75
29	561.25	565.75	57	729.25	733.75

Appendix B - Observed Signal Scatter Ratios, Z_O , for Field Test Cases

Case no.	Wind turbine /unit no(s).	Receiver site / TV channel	Antenna aiming point	$P_{WT,D}$ (dB)	$P_{R,max}$ (dB)	$P_{R,min}$ (dB)	Δ (dB)	m_R	$P_{R,mean}$ (dB)	$F_{A,W}$ (dB)	Z_O (dB)	Z_O (ratio)
7	Mod-1 HAWT	A / 3	Turbine	-27.0	-68.2	-79.3	11.1	0.559	-72.1	0.0	-25.1	0.0031
8	" "	A / 3	Trans.	-27.0	-61.0	-61.5	0.5	0.031	-61.3	-10.8	-26.9	0.0021
9	" "	A / 3	Turbine	-27.0	-74.5	-89.5	15.0	0.695	-79.1	0.0	-27.6	0.0017
10	" "	A / 3	Trans.	-27.0	-64.7	-65.2	0.5	0.031	-65.0	-14.1	-27.1	0.0020
11	" "	A / 8	Turbine	-40.0	-78.0	-82.5	4.5	0.258	-80.0	0.0	-25.9	0.0026
12	" "	A / 8	Trans.	-40.0	-81.3	-84.5	3.2	0.188	-82.8	-2.8	-27.3	0.0019
13	" "	A / 3	Turbine	-31.5	-67.3	-82.2	14.9	0.692	-71.9	0.0	-21.8	0.0066
14	" "	A / 3	Trans.	-31.5	-62.0	-63.5	1.5	0.091	-62.8	-13.7	-19.2	0.0120
15	" "	A / 3	Trans.	-33.9	-68.8	-71.0	2.2	0.131	-69.9	-16.0	-18.8	0.0132
16	" "	A / 5	Turbine	-33.0	-79.5	-100.5	21.0	0.841	-84.8	0.0	-26.7	0.0022
17	" "	A / 7	Turbine	-38.0	-77.8	-78.3	0.5	0.031	-78.1	-18.9	-25.7	0.0027
18	" "	I / 5	Turbine	-33.0	-68.9	-83.5	14.6	0.683	-73.4	0.0	-21.9	0.0065
19	" "	I / 5	Trans.	-33.0	-69.1	-76.9	7.8	0.420	-72.1	-1.3	-22.7	0.0054
20	" "	I / 2	Turbine	-33.0	-84.6	-90.2	5.6	0.314	-87.0	0.0	-32.0	0.0006
22	" "	I / 3	Turbine	-27.0	-78.1	-93.5	15.4	0.707	-82.7	0.0	-29.4	0.0012
23	" "	I / 3	Trans.	-27.0	-78.2	-81.4	3.2	0.188	-79.7	-3.0	-32.1	0.0006
24	" "	I / 8	Turbine	-40.0	-81.0	-90.6	9.6	0.499	-84.5	0.0	-25.3	0.0030
25	" "	I / 8	Trans.	-40.0	-71.6	-72.3	0.7	0.043	-72.0	-12.5	-23.4	0.0046
26	" "	I / 11	Turbine	-40.0	-78.3	-88.7	10.4	0.532	-82.0	0.0	-23.7	0.0042
27	" "	I / 11	Trans.	-40.0	-79.1	-87.1	8.0	0.429	-82.2	0.2	-24.9	0.0032
28	Mod-2 HAWT/No. 2	A / 6	Turbine	50.5	25.5	11.8	13.7	0.653	21.1	0.0	-16.5	0.0221
29	" " "	C / 8	Turbine	33.5	5.2	-0.4	5.6	0.316	2.9	0.0	-20.3	0.0093
30	" " "	C / 6	Turbine	48.5	21.2	19.1	2.1	0.127	20.2	0.0	-23.1	0.0049
31	" " "	A / 19	Turbine	46.0	17.4	9.8	7.6	0.411	14.4	0.0	-19.7	0.0108
32	" " /Nos. 2,3	A / 19	Turbine	28.8	12.8	-2.9	9.9	0.716	8.1	0.0	-11.8	0.0658
	" " */No. 2 only*			*30.0*								
	" " */No. 3 only*			*27.5*								

Appendix B (Cont'd)

Case no.	Wind turbine /unit no(s).	Receiver site / TV channel	Antenna aiming point	$P_{WT,D}$ (dB)	$P_{R,max}$ (dB)	$P_{R,min}$ (dB)	Δ (dB)	m_R	$P_{R,mean}$ (dB)	$F_{A,W}$ (dB)	Z_O (dB)	Z_O (ratio)
33	Mod-2 HAWT/Nos. 1,2,3	A / 19	Turbine	43.2	26.4	10.2	16.2	0.730	21.6	0.0	-12.2	0.0609
	" " */No. 1 only*			*46.5*								
	" " */No. 2 only*			*46.0*								
	" " */No. 3 only*			*27.5*								
34	" " /Nos. 1,2,3	A / 42	Turbine	41.4	25.8	10.1	15.7	0.716	21.1	0.0	-11.6	0.0693
	" " */No. 1 only*			*44.5*								
	" " */No. 2 only*			*45.0*								
	" " */No. 3 only*			*16.5*								
35	" " /Nos. 2,3	B / 12	Turbine	38.1	23.7	20.5	3.2	0.188	22.2	0.0	-15.2	0.0300
	" " */No. 2 only*			*31.0*								
	" " */No. 3 only*			*42.0*								
36	" " /No. 1	C / 6	Turbine	42.0	15.5	13.8	1.7	0.102	14.7	0.0	-23.6	0.0044
37	" " /Nos. 1,3	C / 6	Turbine	42.7	18.3	12.9	5.4	0.304	16.0	0.0	-18.5	0.0141
	" " */No. 1 only*			*38.5*								
	" " */No. 3 only*			*45.5*								
38	17-m Darrieus VAWT	1 / 4	Turbine	-35.4	-48.9	-49.9	1.0	0.061	-49.4	0.0	-19.1	0.0122
39	" " "	1 / 5	Turbine	-33.9	-48.5	-48.8	0.3	0.019	-48.7	0.0	-24.7	0.0034
41	" " "	1 / 13	Turbine	-31.7	-45.5	-46.4	0.9	0.055	-46.0	0.0	-19.7	0.0106
43	" " "	1 / 48	Turbine	-54.8	-74.0	-75.5	1.5	0.091	-74.8	0.0	-20.4	0.0091
44	" " "	2 / 4	Turbine	-35.4	-46.1	-47.1	1.0	0.061	-46.6	0.0	-17.7	0.0168
45	" " "	2 / 5	Turbine	-33.9	-42.7	-43.5	0.8	0.049	-43.1	0.0	-17.7	0.0170
46	" " "	2 / 7	Turbine	-26.2	-38.7	-39.4	0.7	0.043	-39.1	0.0	-20.1	0.0097
47	" " "	2 / 13	Turbine	-31.7	-40.7	-41.8	1.1	0.067	-41.3	0.0	-16.5	0.0222
48	" " "	2 / 23	Turbine	-68.0	-79.9	-81.1	1.2	0.073	-80.5	0.0	-17.6	0.0172
49	" " "	2 / 48	Turbine	-54.8	-75.9	-78.1	2.2	0.131	-77.0	0.0	-19.9	0.0102
50	" " "	3 / 4	Turbine	-35.4	-32.1	-33.1	1.0	0.061	-32.6	0.0	-10.7	0.0845

Appendix B (Cont'd)

Case no.	Wind turbine /unit no(s).	Receiver site / TV channel	Antenna aiming point	$P_{WT,D}$ (dB)	$P_{R,max}$ (dB)	$P_{R,min}$ (dB)	Δ (dB)	m_R	$P_{R,mean}$ (dB)	$F_{A,W}$ (dB)	Z_O (dB)	Z_O (ratio)
51	17-m Darrieus VAWT	3 / 5	Turbine	-33.9	-29.9	-30.7	0.8	0.049	-30.3	0.0	-11.3	0.0740
52	" " "	3 / 7	Turbine	-26.2	-29.8	-30.8	1.0	0.061	-30.3	0.0	-14.2	0.0378
53	" " "	3 / 13	Turbine	-31.7	-37.5	-39.5	2.0	0.120	-38.5	0.0	-12.6	0.0547
54	" " "	3 / 23	Turbine	-68.0	-67.3	-70.9	3.6	0.210	-69.0	0.0	- 7.3	0.1873
55	" " "	3 / 48	Turbine	-54.8	-58.6	-60.9	2.3	0.137	-59.7	0.0	-11.1	0.0779
56	" " "	4 / 4	Turbine	-35.4	-52.4	-57.0	4.6	0.263	-54.4	0.0	-15.3	0.0296
57	" " "	4 / 5	Turbine	-33.9	-46.4	-47.6	1.2	0.073	-47.0	0.0	-17.9	0.0161
58	" " "	4 / 7	Turbine	-26.2	-37.3	-38.2	0.9	0.055	-37.8	0.0	-18.4	0.0145
59	" " "	4 / 13	Turbine	-31.7	-46.1	-48.2	2.1	0.126	-47.1	0.0	-16.7	0.0212
60	" " "	4 / 23	Turbine	-68.0	-78.4	-81.4	3.0	0.177	-79.8	0.0	-13.4	0.0452
61	" " "	4 / 48	Turbine	-54.8	-64.5	-65.1	0.6	0.037	-64.8	0.0	-19.3	0.0116
62	" " "	5 / 4	Turbine	-35.4	-35.3	-36.0	0.7	0.043	-35.7	0.0	-13.8	0.0418
63	" " "	5 / 5	Turbine	-33.9	-35.2	-36.1	0.9	0.055	-35.7	0.0	-13.5	0.0449
64	" " "	5 / 7	Turbine	-26.2	-29.3	-30.3	1.0	0.061	-29.8	0.0	-14.0	0.0401
65	" " "	5 / 13	Turbine	-31.7	-31.9	-33.0	1.1	0.067	-32.5	0.0	-12.1	0.0612
66	" " "	5 / 23	Turbine	-68.0	-72.8	-77.8	5.0	0.284	-75.0	0.0	- 9.0	0.1268
67	" " "	5 / 48	Turbine	-54.8	-56.6	-57.7	1.1	0.067	-57.2	0.0	-12.9	0.0511
68	" " "	6 / 4	Turbine	-35.4	-54.1	-56.1	2.0	0.120	-55.1	0.0	-19.0	0.0125
69	" " "	6 / 5	Turbine	-33.9	-49.9	-58.0	8.1	0.434	-53.0	0.0	-13.2	0.0480
70	" " "	6 / 7	Turbine	-26.2	-33.8	-34.5	0.7	0.043	-34.2	0.0	-17.7	0.0171
71	" " "	6 / 13	Turbine	-31.7	-38.9	-40.1	1.2	0.073	-39.5	0.0	-15.3	0.0296
72	" " "	6 / 23	Turbine	-68.0	-81.3	-85.0	3.7	0.215	-83.0	0.0	-14.2	0.0382
73	" " "	6 / 48	Turbine	-54.8	-68.8	-70.1	1.3	0.079	-69.5	0.0	-18.4	0.0146
74	" " "	7 / 4	Turbine	-35.4	-48.2	-49.8	1.6	0.097	-49.0	0.0	-16.9	0.0203
75	" " "	7 / 5	Turbine	-33.9	-43.3	-44.6	1.3	0.079	-44.0	0.0	-16.1	0.0248
76	" " "	7 / 7	Turbine	-26.2	-36.2	-37.2	1.0	0.061	-36.7	0.0	-17.4	0.0181
77	" " "	7 / 13	Turbine	-31.7	-52.8	-60.9	8.1	0.434	-55.9	0.0	-15.8	0.0266

Appendix B (Concluded)

Case no.	Wind turbine /unit no(s).	Receiver site / TV channel	Antenna aiming point	$P_{WT,D}$ (dB)	$P_{R,max}$ (dB)	$P_{R,min}$ (dB)	Δ (dB)	m_R	$P_{R,mean}$ (dB)	$F_{A,W}$ (dB)	Z_O (dB)	Z_O (ratio)
79	17-m Darrieus VAWT	7 / 48	Turbine	-54.8	-73.6	-75.4	1.8	0.108	-74.5	0.0	-19.5	0.0112
80	" " "	8 / 4	Turbine	-35.4	-52.4	-54.5	3.1	0.126	-53.4	0.0	-18.0	0.0158
81	" " "	8 / 5	Turbine	-33.9	-49.5	-50.6	1.1	0.067	-50.1	0.0	-19.8	0.0104
82	" " "	8 / 7	Turbine	-26.2	-39.1	-39.8	0.7	0.043	-39.5	0.0	-20.3	0.0093
83	" " "	8 / 13	Turbine	-31.7	-44.5	-45.5	1.0	0.061	-45.0	0.0	-18.8	0.0131
84	" " "	8 / 23	Turbine	-68.0	-81.6	-86.2	4.6	0.263	-83.6	0.0	-13.6	0.0434
85	" " "	8 / 48	Turbine	-54.8	-74.2	-75.5	1.3	0.079	-74.9	0.0	-21.1	0.0078

Appendix C - Idealized Signal Scatter Ratios, Z_I, for Field Test Cases

Case no.	Wind turbine /unit no(s).	R (m)	L (m)	A_P (m^2)	$\Delta\beta$ (deg)	θ (deg)	ϕ_S (deg)	Scatter zone	ζ (m)	λ (m)	B_E	$B_{E,\,max}$	Z_I (dB)	Z_I (ratio)
7	Mod-1 HAWT	30.5	30.5	64.2	11.0	9	46	B	1,040	4.56	1.0	2.0	-20.6	0.0086
8	" "	"	"	"	"	"	"	"	"	"	"	"	"	"
9	" "	"	"	"	"	"	"	"	"	"	"	"	"	"
10	" "	"	"	"	"	"	"	"	"	"	"	"	"	"
11	" "	"	"	"	"	"	- 3	"	"	1.61	"	0.8	-17.1	0.0193
12	" "	"	"	"	"	"	"	"	"	"	"	"	"	"
13	" "	"	"	"	"	"	46	"	"	4.56	"	2.0	-20.6	0.0086
14	" "	"	"	"	"	"	"	"	"	"	"	"	"	"
15	" "	"	"	"	"	"	"	"	"	"	"	"	"	"
16	" "	"	"	"	"	"	194	F	"	3.67	1.1	1.7	-19.8	0.0105
17	" "	"	"	"	"	"	97	B	"	1.67	1.0	0.8	-18.9	0.0128
18	" "	"	"	"	"	"	187	F	"	3.67	1.8	1.7	-21.5	0.0071
19	" "	"	"	"	"	"	"	"	"	"	"	"	"	"
20	" "	"	"	"	"	"	-12	B	2,740	5.02	1.1	2.4	-24.9	0.0033
22	" "	"	"	"	"	"	39	"	"	4.56	1.0	2.2	-24.8	0.0033
23	" "	"	"	"	"	"	"	"	"	"	"	"	"	"
24	" "	"	"	"	"	"	-10	"	"	1.61	"	0.8	-21.4	0.0073
25	" "	"	"	"	"	"	"	"	"	"	"	"	"	"
26	" "	"	"	"	"	"	184	F	"	1.47	1.7	0.7	-21.4	0.0073
27	" "	"	"	"	"	"	"	"	"	"	"	"	"	"
28	Mod-2 HAWT/No. 2	45.7	45.7	250.8	6.5	0	30	B	1,600	3.42	2.0	1.2	-17.1	0.0197
29	" " "	"	"	"	"	"	- 3	"	6,100	1.61	"	0.6	-22.7	0.0053
30	" " "	"	"	"	"	"	- 3	"	"	3.42	"	1.2	-22.7	0.0053
31	" " "	"	"	"	"	"	166	F	1,440	0.59	"	0.2	-17.0	0.0199
32	" " /Nos. 2,3												-13.8	0.0420
	" " */No. 2 only*	"	"	"	"	"	*-163*	*F*	*1,600*	"	"	"	*-17.7*	*0.0169*
	" " */No. 3 only*	"	"	"	"	"	*-164*	"	*1,110*	"	"	"	*-16.0*	*0.0251*

Appendix C (Cont'd)

Case no.	Wind turbine /unit no(s).	R (m)	L (m)	A_P (m^2)	$\Delta\beta$ (deg)	θ (deg)	ϕ_S (deg)	Scatter zone	ζ (m)	λ (m)	B_E	$B_{E,\,max}$	Z_I (dB)	Z_I (ratio)
33	Mod-2 HAWT/Nos. 1,2,3												-12.2	0.0598
	" " */No. 1 only*	*45.7*	*45.7*	*250.8*	*8.0*	*0*	*-178*	*F*	*1,800*	*0.59*	*2.0*	*0.2*	*-17.5*	*0.0178*
	" " */No. 2 only*	"	"	"	"	"	*-163*	"	*1,600*	"	"	"	*-17.7*	*0.0169*
	" " */No. 3 only*	"	"	"	"	"	*-164*	"	*1,110*	"	"	"	*-16.0*	*0.0251*
34	" " /Nos. 1,2,3												-11.7	0.0678
	" " */No. 1 only*	"	"	"	"	"	*180*	"	*1,830*	*0.47*	"	"	*-17.5*	*0.0178*
	" " */No. 2 only*	"	"	"	"	"	*164*	"	*1,440*	"	"	"	*-17.2*	*0.0191*
	" " */No. 3 only*	"	"	"	"	"	*175*	"	*1,040*	"	"	"	*-15.1*	*0.0309*
35	" " /Nos. 2,3												-15.4	0.0286
	" " */No. 2 only*	"	"	"	"	"	*154*	"	*1,600*	*1.43*	"	*0.5*	*-19.0*	*0.0126*
	" " */No. 3 only*	"	"	"	"	"	*166*	"	*1,800*	"	"	"	*-18.0*	*0.0160*
36	" " /No. 1	"	"	"	"	"	- 7	B	6,540	1.67	"	1.2	-23.0	0.0050
37	" " /Nos. 1,3												-19.8	0.0105
	" " */No. 1 only*	"	"	"	"	"	*- 7*	"	*6,700*	*3.42*	"	*1.2*	*-23.1*	*0.0049*
	" " */No. 3 only*	"	"	"	"	"	*- 9*	"	*5,800*	"	"	*1.2*	*-22.5*	*0.0056*
38	17-m Darrieus VAWT	8.5	24.1	14.7	0.0	0	90	B	125	4.18	2.0	2.0	-22.6	0.0055
39	" " "	"	"	"	"	"	"	"	"	3.67	"	"	"	"
41	" " "	"	"	"	"	"	"	"	"	1.39	"	"	"	"
43	" " "	"	"	"	"	"	"	"	"	0.44	"	"	"	"
44	" " "	"	"	"	"	"	0	"	37	4.18	"	"	-18.9	0.0130
45	" " "	"	"	"	"	"	"	"	"	3.67	"	"	"	"
46	" " "	"	"	"	"	"	"	"	"	1.67	"	"	"	"
47	" " "	"	"	"	"	"	"	"	"	1.39	"	"	"	"
48	" " "	"	"	"	"	"	"	"	"	0.57	"	"	"	"
49	" " "	"	"	"	"	"	"	"	"	0.44	"	"	"	"
50	" " "	"	"	"	"	"	180	F	29	4.18	"	"	-13.5	0.0448

Appendix C (Cont'd)

Case no.	Wind turbine /unit no(s).	R (m)	L (m)	A_P (m^2)	$\Delta\beta$ (deg)	θ (deg)	ϕ_S (deg)	Scatter zone	ζ (m)	λ (m)	B_E	$B_{E,\,max}$	Z_I (dB)	Z_I (ratio)
51	17-m Darrieus VAWT	8.5	24.1	14.7	0.0	0	180	F	29	3.67	2.0	2.0	-13.5	0.0448
52	" " "	"	"	"	"	"	"	"	"	1.67	"	"	"	"
53	" " "	"	"	"	"	"	"	"	"	1.39	"	"	"	"
54	" " "	"	"	"	"	"	"	"	"	0.57	"	"	"	"
55	" " "	"	"	"	"	"	"	"	"	0.44	"	"	"	"
56	" " "	"	"	"	"	"	0	B	33	4.18	"	"	-15.3	0.0294
57	" " "	"	"	"	"	"	"	"	"	3.67	"	"	"	"
58	" " "	"	"	"	"	"	"	"	"	1.67	"	"	"	"
59	" " "	"	"	"	"	"	"	"	"	1.39	"	"	"	"
60	" " "	"	"	"	"	"	"	"	"	0.57	"	"	"	"
61	" " "	"	"	"	"	"	"	"	"	0.44	"	"	"	"
62	" " "	"	"	"	"	"	180	F	18	4.18	"	"	-11.5	0.0711
63	" " "	"	"	"	"	"	"	"	"	1.39	"	"	"	"
64	" " "	"	"	"	"	"	"	"	"	1.39	"	"	"	"
65	" " "	"	"	"	"	"	"	"	"	1.39	"	"	"	"
66	" " "	"	"	"	"	"	"	"	"	1.39	"	"	"	"
67	" " "	"	"	"	"	"	"	"	"	1.39	"	"	"	"
68	" " "	"	"	"	"	"	100	B	21	4.18	"	"	-15.2	0.0302
69	" " "	"	"	"	"	"	"	"	"	3.67	"	"	"	"
70	" " "	"	"	"	"	"	"	"	"	1.67	"	"	"	"
71	" " "	"	"	"	"	"	"	"	"	1.39	"	"	"	"
72	" " "	"	"	"	"	"	"	"	"	0.57	"	"	"	"
73	" " "	"	"	"	"	"	"	"	"	0.44	"	"	"	"
74	" " "	"	"	"	"	"	45	"	24	4.18	"	"	-14.2	0.0379
75	" " "	"	"	"	"	"	"	"	"	3.67	"	"	"	"
76	" " "	"	"	"	"	"	"	"	"	1.67	"	"	"	"
77	" " "	"	"	"	"	"	"	"	"	1.39	"	"	"	"

Appendix C (Concluded)

Case no.	Wind turbine /unit no(s).	R (m)	L (m)	A_P (m^2)	$\Delta\beta$ (deg)	θ (deg)	ϕ_S (deg)	Scatter zone	ζ (m)	λ (m)	B_E	$B_{E,\,max}$	Z_I (dB)	Z_I (ratio)
79	17-m Darrieus VAWT	8.5	24.1	14.7	0.0	0	45	B	24	0.44	2.0	2.0	-14.2	0.0379
80	" " "	"	"	"	"	"	135	"	23	4.18	"	"	-17.8	0.0165
81	" " "	"	"	"	"	"	"	"	"	3.67	"	"	"	"
82	" " "	"	"	"	"	"	"	"	"	1.67	"	"	"	"
83	" " "	"	"	"	"	"	"	"	"	1.39	"	"	"	"
84	" " "	"	"	"	"	"	"	"	"	0.57	"	"	"	"
85	" " "	"	"	"	"	"	"	"	"	0.44	"	"	"	"

REPORT DOCUMENTATION PAGE

Form Approved
OMB No. 0704-0188

1. AGENCY USE ONLY (*Leave blank*)	2. REPORT DATE	3. REPORT TYPE AND DATES COVERED
	May 1994	Final Contractor Report

4. TITLE AND SUBTITLE

Equations for Estimating the Strength of TV Signals Scattered by Wind Turbines

5. FUNDING NUMBERS

WU–505–63–5B
C–NAS3–25266

6. AUTHOR(S)

David A. Spera and Dipak L. Sengupta

7. PERFORMING ORGANIZATION NAME(S) AND ADDRESS(ES)

Sverdrup Technology, Inc.
Lewis Research Center Group
2001 Aerospace Parkway
Brook Park, Ohio 44142

8. PERFORMING ORGANIZATION REPORT NUMBER

E–8579

9. SPONSORING/MONITORING AGENCY NAME(S) AND ADDRESS(ES)

National Aeronautics and Space Administration
Lewis Research Center
Cleveland, Ohio 44135–3191

10. SPONSORING/MONITORING AGENCY REPORT NUMBER

NASA CR–194468

11. SUPPLEMENTARY NOTES

David A. Spera, Sverdrup Technology, Inc., Brook Park, Ohio 44142 (work funded by NASA Contract NAS3–25266), presently at NYMA, Inc., Engineering Services Division, Brook Park, Ohio 44142; Dipak L. Sengupta, University of Detroit Mercy, Detroit, Michigan 48221. Project Manager, M.H. Hirschberg, Structures Division, organization code 5200, NASA Lewis Research Center, (216) 433–3206.

12a. DISTRIBUTION/AVAILABILITY STATEMENT

Unclassified - Unlimited
Subject Category 34

12b. DISTRIBUTION CODE

13. ABSTRACT ***(Maximum 200 words)***

During the late 1970's and early 1980's, concerns about the potential interference of wind turbine generators with electromagnetic communication signals led to a series of research studies, both in the laboratory and in the field, conducted by the staff of the University of Michigan Radiation Laboratory. These studies were sponsored by organizations such as the U.S. Department of Energy (Refs. 1-7), the Solar Energy Research Institute (Refs. 5-8), and private developers of wind power stations (Refs. 9 and 10). Research objectives were to identify the mechanisms by which wind turbines might adversely affect communication signals, estimate the severity of these effects for different types of signals (e.g. television, radio, microwave, and navigation), and formulate mathematical models with which to predict the sizes of potential interference zones around wind turbines and wind power plants. This work formed the basis for preliminary standards on assessing electromagnetic interference (EMI) by wind turbines (Ref. 11). With the current renewal of interest in wind energy projects, it is appropriate that the many experimental and analytical aspects of this pioneering work be reviewed and correlated. The purpose of this study is to combine test data and theory from previously published and unpublished research reports into a unified and consistent set of equations which are useful for estimating potential levels of television interference from wind turbines. To be comprehensive, these equations will include both horizontal-axis and vertical-axis wind turbines (HAWTs and VAWTs), blade configuration parameters (e.g. number, size, material, twist, and coning), signal frequency and power, and directional characteristics of the receiving antenna. The approach that is followed in this report is as follows: First, some basic equations that describe electromagnetic signals with interference are presented without detailed derivations, since the latter are available in the references. Minor changes in terminology are made for purposes of consistency. Next, the concept of a signal scatter ratio is introduced, which defines the fraction of the signal impinging on a wind turbine that is scattered by its blades onto a nearby receiver. Equations from references are modified for the calculation of experimental scatter ratios (from measured signals containing interference) and idealized scatter ratios (from rotor characteristics and relative locations of the transmitter, the turbine, and the receiver). Experimental and idealized scatter ratios are then calculated and compared for 75 cases from the literature, in which TVI measurements were made around a variety of wind turbines (Fig. 1). An empirical equation is then defined for estimating the probability that an actual scatter ratio will differ from an idealized ratio by a given amount. Finally, a sample calculation of the size of a potential TV interference zone around a hypothetical wind power station is presented.

14. SUBJECT TERMS	15. NUMBER OF PAGES
Wind turbine; Wind energy; Signal interference	33
	16. PRICE CODE: A03

17. SECURITY CLASSIFICATION OF REPORT	18. SECURITY CLASSIFICATION OF THIS PAGE	19. SECURITY CLASSIFICATION OF ABSTRACT	20. LIMITATION OF ABSTRACT
Unclassified	Unclassified	Unclassified	

National Aeronautics and
Space Administration

Lewis Research Center
21000 Brookpark Rd.
Cleveland, OH 44135-3191